NANO LETTERS

Letter

pubs.acs.org/NanoLett

Metastability in Pressure-Induced Structural Transformations of CdSe/ZnS Core/Shell Nanocrystals

Michael Grünwald,*[,†] Katie Lutker,[†] A. Paul Alivisatos,[†,‡] Eran Rabani,[§] and Phillip L. Geissler[†,‡]

[†]Department of Chemistry, University of California, Berkeley, California 94720, United States

[‡]Materials Sciences Division, Lawrence Berkeley National Laboratories, Berkeley, California 94720, United States

[§]School of Chemistry, The Sackler Faculty of Exact Sciences, Tel Aviv University, Tel Aviv 69978, Israel

Supporting Information

ABSTRACT: The kinetics and thermodynamics of structural transformations under pressure depend strongly on particle size due to the influence of surface free energy. By suitable design of surface structure, composition, and passivation it is possible, in principle, to prepare nanocrystals in structures inaccessible to bulk materials. However, few realizations of such extreme size-dependent behavior exist. Here, we show with molecular dynamics computer simulation that in a model of CdSe/ZnS core/shell nanocrystals the core high-pressure structure can be made metastable under ambient conditions by tuning the thickness of the shell. In nanocrystals with thick shells, we furthermore observe a wurtzite to NiAs transformation, which does not occur in the pure bulk materials. These phenomena are linked to a fundamental change in the atomistic transformation mechanism from heterogeneous nucleation at the surface to homogeneous nucleation in the crystal core.

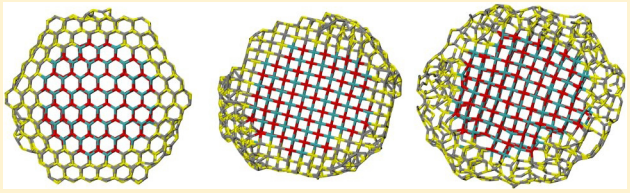

KEYWORDS: *Core/shell nanocrystals, structural transformation, metastability, nucleation, molecular simulation*

At thermodynamic equilibrium, matter adopts the form that minimizes its total free energy.[1] Close to first-order phase transitions, however, metastability of the competing phases is often observed; liquid water can be cooled many degrees below its freezing point, magnets can withstand oppositely oriented magnetic fields, and diamonds do not transform to graphite at ambient conditions. How far one can push a system out of its equilibrium phase depends on the microscopic transformation mechanism that determines the height of the free energy barrier separating the competing phases.

Exploiting the metastability of different solid phases is a possible route to creating materials with new properties. However, many crystal structures form only when high pressure is applied and are unstable under ambient conditions in the bulk. On the other hand, in nanocrystals phase diagrams and microscopic transformation mechanisms can depend strongly on particles' size and shape.[2−6] The wurtzite to rocksalt transformation in CdSe nanocrystals, for example, shows an increasing thermodynamic transition pressure and a decreasing activation enthalpy with decreasing particles size.[3,7−9] While it is in principle possible to extend the metastability of high-pressure structures to ambient conditions by engineering the surface properties of nanoparticles,[5,10−12] significant insight into the underlying microscopic transformation dynamics is required.

A particularly interesting surface modification is realized in core/shell nanocrystals,[13] where the core material is epitaxially overgrown with a material of identical crystal structure.[14−16] While the optical qualities of these heteromaterials are well-studied,[17] little is known about their structural properties.[18] In modern synthesis methods, materials with a lattice mismatch of up to 11% can be combined to form a pristine core/shell interface.[17] The resulting lattices of both core and shell experience a strong strain that depends sensitively on particle size and has the potential of introducing dramatic changes to the nanoparticle's structural and kinetic behavior under pressure.

In this Letter, we report the simulation of spherical wurtzite CdSe nanocrystals of 3 nm diameter (≈500 atoms), that have been epitaxially passivated with ZnS shells of thicknesses up to 2.1 nm (5 monolayers, see Supporting Information). The largest of these core/shell crystals consists of ≈7000 atoms. The particles are modeled with empirical pair potentials designed to reproduce a number of properties of the bulk materials.[19−21] In our simulations, a single crystal is immersed in a pressure bath of ideal gas particles[22,23] at a temperature of 300 K and the pressure is increased in steps of 0.2 GPa every 10 ps.[25] These pressurization rates are many orders of magnitude larger than in experiments using diamond anvil cells but are comparable to recent shock-wave experiments on CdSe nanocrystals.[26] When a pressure of 20 GPa is reached after 1 ns, the pressure is released again at the same rate. After reaching ambient pressures, the crystals are simulated for another 2 ns. For the largest crystals, more than 800 000 gas particles need to be simulated at the maximum pressure of 20

Received: February 21, 2012
Revised: July 6, 2012
Published: July 16, 2012

dx.doi.org/10.1021/nl3007165 | *Nano Lett.* 2013, 13, 1367−1372

GPa. We monitor the evolution of the crystal structure by calculating atom-coordination numbers based on the radial pair distribution functions of core and shell atoms.

The effect of the ZnS shell on the structure of the CdSe core is dramatic. In Figure 1B we plot the density of the wurtzite

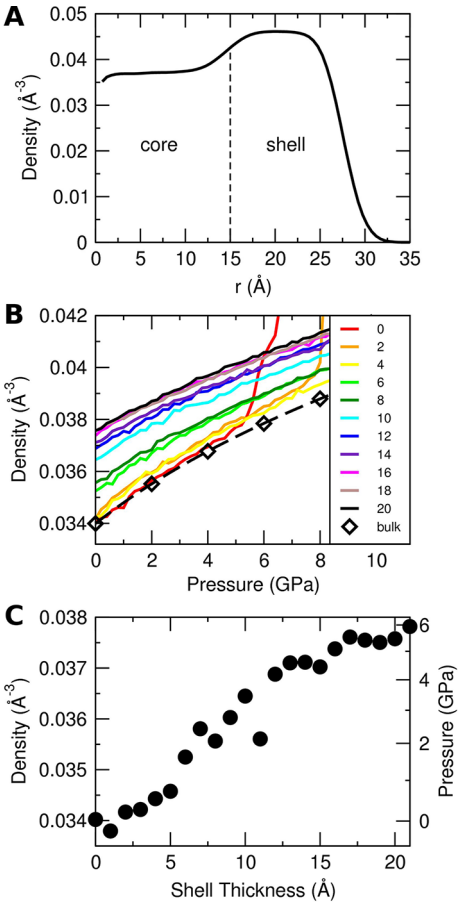

Figure 1. The ZnS shell compresses the CdSe core. (A) Coarse-grained atom density of a 1.5 nm shell-crystal at zero pressure as a function of distance r from the center of mass (see Supporting Information). The different densities of the core and shell materials are well visible. (B) Density of the core as a function of pressure, for nanocrystals with different shell thickness (legend values indicate shell thickness in Å). The density of bulk CdSe, obtained from constant pressure Monte Carlo simulations, is shown for reference. The dashed line is a fit of the bulk data to the Murnaghan equation of state. Note that the sudden increase in density observed for 0 and 0.2 nm shell-crystals is a signature of the wurtzite to rocksalt transformation. (C) Core density at zero pressure as a function of shell thickness. The right-hand ordinate shows the pressure necessary to achieve equivalent densities in bulk CdSe.

core of crystals with different shell sizes as a function of external pressure. The density of the core increases significantly with increasing shell thickness. For a 2 nm shell, this compression effect is equivalent to an additional external pressure of 6 GPa, as illustrated in Figure 1C. This pressure is much higher than the bulk coexistence pressure of 2.4 GPa of our CdSe model, and high enough to cause spontaneous transformation in bare CdSe crystals. Similarly high pressures were found at the core/shell interface in experiments of CdS/ZnS nanocrystals.[27] One might therefore expect the transformation in core/shell crystals to happen at lower pressures compared to bare CdSe nanocrystals. Quite to the contrary, the upstroke transformation pressure of the core increases strongly with increasing shell size, as illustrated in Figure 2. While pure CdSe nanocrystals transform at around 6 GPa, transformation pressures of up to 18 GPa are observed for crystals with thick shells.

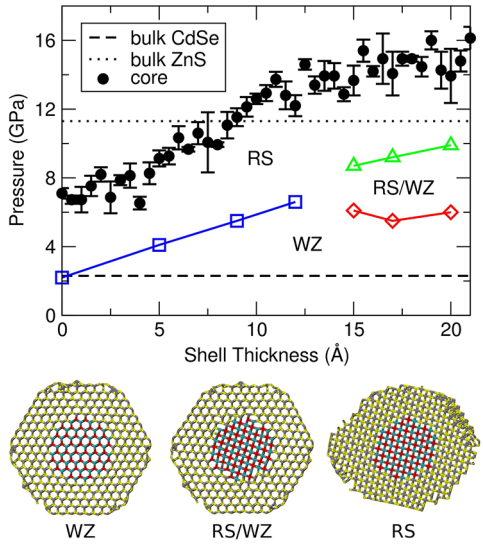

Figure 2. Size-dependent transformation pressure. Core upstroke transformation pressures (solid black circles) are plotted as a function of shell thickness.[24] At these pressures, the fraction of six-coordinated atoms exceeds 0.1 for the first time. The thermodynamic transition pressure of bulk CdSe (dashed line) and bulk ZnS (dotted line) are shown for reference. Points of equal enthalpy (blue squares and red diamonds), obtained from constant pressure Monte Carlo simulations, give an estimate of the nanocrystal phase diagram as a function of shell thickness. The three phases are illustrated below the graph as cross sections of a 2 nm shell crystal: wurtzite core and shell (WZ), a rocksalt core in a wurtzite shell (RS/WZ), and rocksalt core and shell (RS).

Our simulations suggest that the increase in upstroke transformation pressure with particle size is caused by an increase in thermodynamic transition pressure and a concurrent removal of favorable surface nucleation sites. We estimated the phase diagram of the nanoparticles by calculating the pressures at which crystals in different phases have equal enthalpy (see Figure 2).[28] In particular, we consider three combinations of core/shell crystal structures: wurtzite/wurtzite (WZ), rocksalt/wurtzite (RS/WZ), and rocksalt/rocksalt (RS). A shell thickness of 0.5 nm, corresponding to a single monolayer of ZnS, is enough to raise the thermodynamic transition pressure by 2 GPa. With increasing shell size, the phase boundary of RS approaches the bulk thermodynamic transition pressure of our ZnS model. At larger shell sizes (3−4 monolayers), the mixed phase RS/WZ, featuring distinct crystal structures in the core and shell, appears as a stable intermediate between the homogeneous phases. The thermodynamic transformation pressure from WZ to RS/WZ is fairly insensitive to shell thickness, indicating that a large-shell regime has been reached. This conclusion is corroborated by the observed upstroke transformation pressures that are approximately constant in this size regime.

Computer simulations of pure CdSe nanocrystals have shown that transformations are initiated via nucleation events on the surface.[8,9] While we observe similar surface nucleation in core/shell crystals with shell thicknesses up to 3 monolayers,

dx.doi.org/10.1021/nl3007165 | *Nano Lett.* 2013, 13, 1367−1372

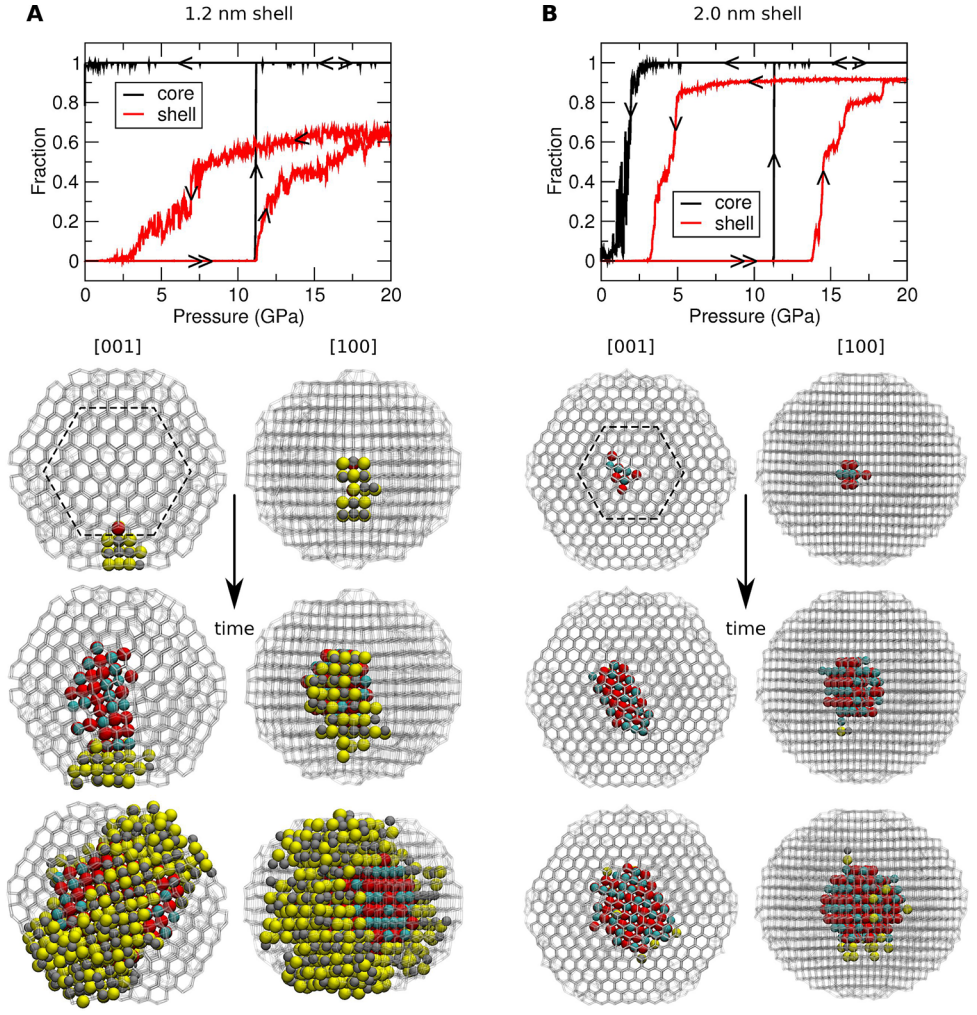

Figure 3. The nucleation mechanism changes with increasing shell thickness. (A) Fraction of 6-coordinated atoms as a function of pressure in the core (black) and shell (red) of a 1.2 nm shell crystal. The transformation of both core and shell start around 11 GPa. Cross sections highlight stages of the nucleation process, as seen along the [001] and [100] directions. The dashed line marks the interface between core and shell. Atoms that have undergone a change of coordination are shown opaque. (For clarity, only clusters of 10 atoms or more are shown.) The transformation nucleates at the crystal surface and propagates inward. (B) Fraction of 6-coordinated atoms of a 2 nm shell crystal. The transformations of the core and shell happen at different pressures, around 11 and 14 GPa, respectively. Snapshots show that the nucleus is located in the core.

for crystals with thick shells nucleation happens in the core, as illustrated in Figure 3 and Supporting Videos 1 and 2. This fundamental change of nucleation mechanism can be rationalized based on the estimated phase diagram in Figure 2. For shell thicknesses larger than ≈1.2 nm, the mixed phase RS/WZ is stable at intermediate pressures with respect to the two pure phases. At higher pressures, one expects the mixed phase to remain stable with respect to the lower density WZ structure, while becoming less stable than the denser RS phase. This ordering of free energies, according to Ostwald's step rule, makes likely the appearance of RS/WZ en route from WZ to RS for shells in this size range. The ordering of free energies for smaller particles is less clear. Since the stability of RS/WZ with respect to WZ at high pressures likely continues beyond the size range where RS/WZ is a thermodynamic minimum, the change in transformation mechanism can be expected to occur for shells slightly thinner than the estimated triple point thickness. In any case, the barrier for nucleation on the surface will depend strongly on the particular surface configuration of the crystal. Indeed, for shell sizes in the triple point region, we observe variation in nucleation mechanism among independent simulation runs.

While a typical core transformation event lasts no longer than 10 ps, transformations of shells proceed in steps, creating only confined regions of rocksalt at a time. The hysteresis curves[29] in Figure 3 manifest such dynamics. By 20 GPa, however, most shells have completed the transformation to rocksalt. By comparison, we found that a pure 4 nm ZnS nanocrystal remained in the wurtzite structure when subjected to the same pressure protocol, indicating that the core also influences the shell. Upon release of pressure, all crystal shells undergo a back-transformation: thick shells transform back to a mixture of wurtzite/zinc-blende and thin shells transform back to predominantly amorphous four-coordinated structures.

On the other hand, crystal cores did not all undergo a back-transformation. While cores with thin shells ($\lesssim$1 monolayers) and thick shells ($\gtrsim$4 monolayers) transform back to mixtures of wurtzite and zinc-blende structures, cores in a broad range of intermediate shell sizes remain in the rocksalt structure down to zero pressure, as illustrated in Figure 4. This nonmonotonic behavior is related to the interface between the rocksalt core

dx.doi.org/10.1021/nl3007165 | *Nano Lett.* 2013, 13, 1367−1372

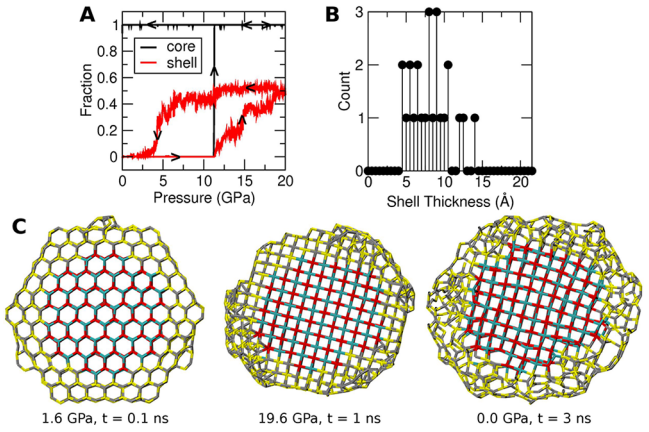

Figure 4. Rocksalt metastability at ambient pressure. (A) Fraction of 6-coordinated atoms in the core (black) and shell (red) of a 0.9 nm shell crystal as the pressure is increased to 20 GPa and then released again. The rocksalt to wurtzite transformation at around 11 GPa is well visible. While the shell undergoes the back-transformation at around 5 GPa, the core remains in the rocksalt structure even at zero pressure. (B) Number of trajectories (from a total of 3) for which the fraction of 6-coordinated atoms in the core exceeded 90%, 2 ns after completing the pressure cycle. While crystals with very thin (<0.4 nm) and thick (>1.5 nm) shells transform back, crystals in a range of intermediate shell thicknesses can remain in the rocksalt structure. (C) Cross sections of a 0.9 nm shell crystal at different points in the pressure cycle, viewed along the wurtzite *c*-axis. (Left) At an upstroke pressure of 1.6 GPa, both core and shell are in the wurtzite structure. (Middle) At 19.6 GPa, the crystal is in the rocksalt structure. (Right) A nanosecond after completing the pressure cycle, the rocksalt structure in the core persists. The shell has transformed back into a predominantly amorphous 4-coordinated structure.

and the retransformed shell. For shells thinner than 1 monolayer, the amount of ZnS is too low to form a contiguous shell and core dynamics are not strongly influenced. Shells with intermediate thicknesses transform back into amorphous 4-coordinated structures that neatly passivate the rocksalt core, remove favorable nucleation sites at the core−shell interface, and therefore suppress structural rearrangements within the core as pressure is reduced. Very thick shells, however, transform back into crystalline wurtzite/zinc-blende mixtures that are incommensurate with the rocksalt structure of the core. The induced stress at the core/shell interface facilitates the back-transformation of the core. A set of simulations that corroborate the important role of the core/shell interface are illustrated in Supporting Information Figures 1 and 2.

To estimate the lifetime of metastable rocksalt cores, we have performed long zero pressure simulations at a temperature of 600 K, starting from configurations with metastable rocksalt cores. As expected, the size regime over which metastability can be observed under these conditions narrows. However, crystals with a shell thickness of 0.9 nm did not transform back even after 90 ns of molecular dynamics at 600 K. Assuming a fundamental molecular time scale of 0.5 ps (a typical phonon period), we estimate the free energy barrier to be larger than 16 k_BT at room temperature, and the corresponding time scale for the transformation longer than 13 ms. In fact, recent experiments suggest substantial metastability on time scales much longer than that.[18]

Phase transitions that occur far from equilibrium do not necessarily lead to the phase with the lowest free energy. In fact, Ostwald's step rule predicts that a system will transform from a metastable phase to the phase with the smallest free energy difference. In an unexpected realization of this rule of thumb, we observed a wurtzite to NiAs (B8) transformation in a few crystals with thick shells. Figure 5A shows three snapshots of a 1.9 nm shell crystal. In the course of the transformation a grain boundary between the expected rocksalt structure and the NiAs structure builds up in the core and later propagates into the

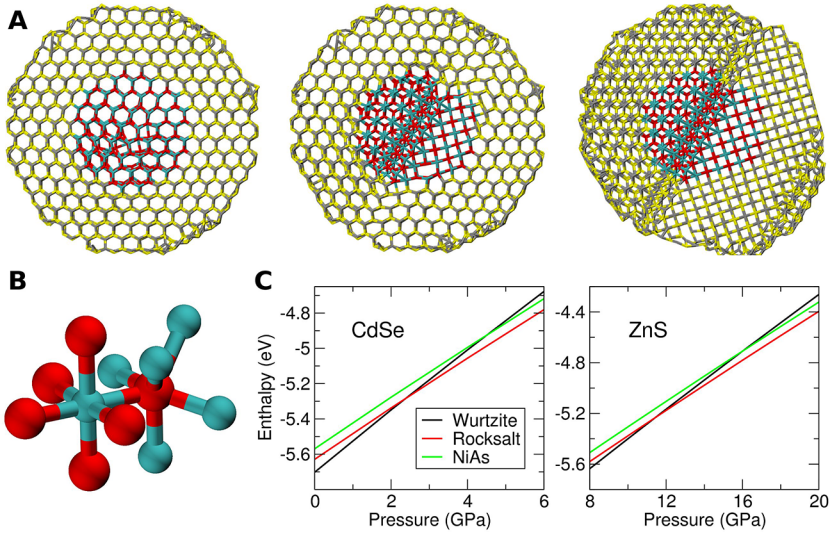

Figure 5. NiAs structure nucleates at high pressures. (A) Time series of cross sections of a 1.9 nm shell nanocrystal undergoing transforming from wurtzite to NiAs/rocksalt. The crystal is viewed along the wurtzite *c*-axis and the same set of atoms is displayed throughout. (Left) First stage of nucleation in the core at 17 GPa. (Center) Four picoseconds later, no 4-coordinated atoms remain in the core and a grain boundary between NiAs (upper left part of the crystal) and rocksalt (lower right part) is visible. The shell is visibly strained but is still wurtzite. (Right) At 20 GPa, no four-coordinated atoms remain; the NiAs grain-boundary spans the entire crystal. (B) Close-up view of a patch of CdSe in the NiAs structure, highlighting the different coordination environments of Cd (blue) and Se (red) atoms. (C) Bulk enthalpies per atom as a function of pressure for CdSe and ZnS in the wurtzite, rocksalt, and NiAs structures. Throughout the pressure range studied (0−20 GPa), NiAs is never stable. It is metastable with respect to the wurtzite structure at pressures larger than 4.5 and 16 GPa for CdSe and ZnS, respectively.

dx.doi.org/10.1021/nl3007165 | *Nano Lett.* 2013, 13, 1367−1372

shell at higher pressures. Like rocksalt, the NiAs structure is 6-coordinated. Cations are in a rocksalt-type coordination environment, while anions are coordinated by a trigonal prism of cations (Figure 5B). The occurrence of the NiAs structure is surprising, since it has not been observed experimentally in the pure materials, neither in the bulk nor in nanocrystals. Figure 5C shows a plot of the bulk enthalpies of the core and shell materials in the wurtzite, rocksalt, and NiAs structures as a function of pressure.[30] Throughout the pressure range studied here (0–20 GPa), NiAs is never enthalpically most stable. However, it becomes metastable with respect to the wurtzite structure at pressures larger than 4.5 and 16 GPa for CdSe and ZnS, respectively. (The transformation illustrated in Figure 5C occurred at 17 GPa.) Interestingly, in a recent pressure study of ZnS/CdSe core/shell nanocrystals an unexpected Raman peak was observed after the transformation had happened.[31]

In summary, we have shown that both the kinetics and thermodynamics of the wurtzite to rocksalt transformation in CdSe/ZnS core/shell crystals are strongly affected by the thickness of the shell. A strong increase in thermodynamic transition pressure with increasing shell thickness is accompanied by a substantial broadening of the hysteresis, rendering the transformed rocksalt cores metastable at ambient conditions. The upstroke nucleation pathway changes from heterogeneous nucleation on the surface to homogeneous nucleation in the core. In thick-shell crystals, the greatly increased upstroke transformation pressure can lead to nucleation of the NiAs structure, which is not observed in the two pure materials.

The unexpected occurrence of a new high-pressure NiAs structure suggests that other materials might be susceptible to a similar phenomenon. By artificially increasing the pressures at which solid–solid transformation take place, transformation routes to other, previously unobservable crystal structures might become available. Potentially, such an increase can be achieved by blocking favorable nucleation pathways through suitable surface modifications, or by using high pressurization rates as obtained in shockwave experiments.

■ ASSOCIATED CONTENT

Supporting Information

Additional methods, figures, and videos. This material is available free of charge via the Internet at http://pubs.acs.org.

■ AUTHOR INFORMATION

Corresponding Author

*E-mail: michael.gruenwald@berkeley.edu.

Notes

The authors declare no competing financial interest.

■ ACKNOWLEDGMENTS

We thank Christoph Dellago for useful discussions. This work was supported by the FP7Marie Curie IOF project HJSC. E.R. thanks the Miller Institute for Basic Research in Science at UC Berkeley for partial financial support via a Visiting Miller Professorship. M.G. was supported by the Austrian Science Fund (FWF) under Grant J 3106-N16. K.L. and A.P.A. acknowledge funding by the Self-Assembly of Organic/Inorganic Nancomposite Materials, which is supported by the Director, Office of Science, Office of Basic Energy Sciences of the U.S. Department of Energy under Contract No. DE-AC02-05CH11231.

■ REFERENCES

(1) Callen, H. B. *Thermodynamics and an Introduction to Thermostatistics*, 2nd ed.; John Wiley & Sons: New York, 1985.
(2) Tolbert, S. H.; Alivisatos, A. P. *Science* **1994**, *265*, 373–376.
(3) Chen, C.-C.; Herhold, A. B.; Johnson, C. S.; Alivisatos, A. P. *Science* **1997**, *276*, 398.
(4) Jacobs, K.; Zaziski, D.; Scher, E. C.; Herhold, A. B.; Alivisatos, A. P. *Science* **2001**, *293*, 1803.
(5) Grünwald, M.; Rabani, E.; Dellago, C. *Phys. Rev. Lett.* **2006**, *96*, 255701.
(6) Bealing, C.; Fugallo, G.; Martonak, R.; Molteni, C. *Phys. Chem. Chem. Phys.* **2010**, *12*, 8542–8550.
(7) Tolbert, S. H.; Alivisatos, A. P. *J. Chem. Phys.* **1995**, *102*, 4642.
(8) Grünwald, M.; Dellago, C. *Nano Lett.* **2009**, *9*, 2099–102.
(9) Grünwald, M.; Dellago, C. *J. Chem. Phys.* **2009**, *131*, 164116.
(10) Farvid, S. S.; Dave, N.; Wang, T.; Radovanovic, P. V. *J. Phys. Chem. C* **2009**, *113*, 15928–15933.
(11) Jacobs, K.; Wickham, J.; Alivisatos, A. P *J. Phys. Chem. B* **2002**, *106*, 3759.
(12) Dinega, D. P.; Bawendi, M. G. *Angew. Chem., Int. Ed.* **1999**, *38*, 1788–1791.
(13) Spanhel, L.; Haase, M.; Weller, H.; Henglein, A. *J. Am. Chem. Soc.* **1987**, *109*, 5649–5655.
(14) Hines, M. A.; Guyot-Sionnest, P. *J. Phys. Chem.* **1996**, *100*, 468.
(15) Dabbousi, B. O.; Rodriguez-Viejo, J.; Mikulec, F. V.; Heine, J. R.; Mattoussi, H.; Ober, R.; Jensen, K. F.; Bawendi, M. G. *J. Phys. Chem. B* **1997**, *101*, 9463–9475.
(16) Peng, X.; Schlamp, M. C.; Kadavanich, A. V.; Alivisatos, A. P. *J. Am. Chem. Soc.* **1997**, *119*, 7019–7029.
(17) Rosenthal, S.; Mcbride, J.; Pennycook, S.; Feldman, L. *Surf. Sci. Rep.* **2007**, *62*, 111–157.
(18) Li, Z.; Wang, L.; Liu, B.; Wang, J.; Liu, B.; Li, Q.; Zou, B.; Cui, T.; Meng, Y.; Mao, H.-k.; Liu, Z.; Liu, J. *Phys Status Solidi B* **2011**, *248*, 1149–1153.
(19) Rabani, E. *J. Chem. Phys.* **2001**, *115*, 1493.
(20) Rabani, E. *J. Chem. Phys.* **2002**, *116*, 258.
(21) Grünwald, M.; Zayak, A.; Neaton, J. B.; Rabani, E.; Geissler, P. L. *J. Chem. Phys.* **2012**, *136*, 234111.
(22) Grünwald, M.; Dellago, C. *Mol. Phys.* **2006**, *104*, 3709.
(23) Grünwald, M.; Geissler, P. L.; Dellago, C. *J. Chem. Phys.* **2007**, *127*, 154718.
(24) Data points are averages over three independent simulation runs per nanocrystal size; error bars indicate one standard deviation.
(25) The equations of motion were integrated with the velocity Verlet algorithm[32] and a time step of 2 fs. The ideal gas barostat was parametrized as in ref 23.
(26) Wittenberg, J.; Merkle, M.; Alivisatos, A. P. *Phys. Rev. Lett.* **2009**, *103*, 1–4.
(27) Ithurria, S.; Guyot-Sionnest, P.; Mahler, B.; Dubertret, B. *Phys. Rev. Lett.* **2007**, *99*, 265501.
(28) Points of equal enthalpy were determined in NPT-Monte Carlo simulations as described in ref 9. Initial configurations were extracted from the molecular dynamics trajectories in which the transformations were observed.
(29) The fractions of 4- and 6-coordinated atoms in Figures 3 and 4 were calculated as follows: For every configuration along a given trajectory, the radial pair distribution function $g(r)$ was calculated separately for core and shell atoms and averaged over 5 ps intervals. The first minimum of $g(r)$ was found numerically and the respective distance used as a cutoff for the calculation of the number of nearest neighbors. To minimize interfacial contributions, only core atoms within 10 Å of the center of mass were included in the calculation; likewise, shell atoms within 18 Å of the center were excluded.
(30) Bulk enthalpies were calculated in NPT-Monte Carlo simulations of approximately 500 periodically replicated atoms.

Ewald sums were used for the calculation of electrostatic interactions.[32]

(31) Fan, H. M.; Ni, Z. H.; Feng, Y. P.; Fan, X. F.; Kuo, J. L.; Shen, Z. X.; Zou, B. S. *Appl. Phys. Lett.* **2007**, *90*, 021921.

(32) Frenkel, D.; Smit, B. *Understanding Molecular Simulation*; Academic Press: New York, 2002.